Acta Crystallographica Section F
Structural Biology and Crystallization Communications
ISSN 1744-3091

Crystallization and preliminary X-ray crystallographic studies of succinic semialdehyde dehydrogenase from *Streptococcus pyogenes*

Eun Hyuk Jang,[a]‡ Jong Eun Lim,[b]‡ Young Min Chi[a] and Ki Seog Lee[b]*

[a]Division of Biotechnology, College of Life Sciences and Biotechnology, Korea University, Seoul 136-713, Republic of Korea, and [b]Department of Clinical Laboratory Science, College of Health Sciences, Catholic University of Pusan, Busan 609-757, Republic of Korea

‡ These authors contributed equally to this study.

Correspondence e-mail: kslee@cup.ac.kr

Received 1 November 2011
Accepted 2 December 2011

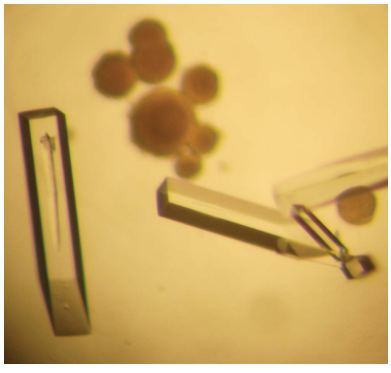

Succinic semialdehyde dehydrogenase (SSADH) plays a critical role in the metabolism of the inhibitory neurotransmitter γ-aminobutyric acid (GABA) and catalyzes the NAD(P)$^+$-coupled oxidation of succinic semialdehyde (SSA) to succinic acid (SA). SSADH from *Streptococcus pyogenes* has been purified and crystallized as the apoenzyme and in a complex with NAD$^+$. The crystals of native and NAD$^+$-complexed SSADH diffracted to resolutions of 1.6 and 1.7 Å, respectively, using a synchrotron-radiation source. Both crystals belonged to the orthorhombic space group $P2_12_12_1$, with unit-cell parameters a = 93.3, b = 100.3, c = 105.1 Å for the native crystal and a = 93.3, b = 100.3, c = 105.0 Å for the complex crystal. Preliminary molecular replacement confirmed the presence of one dimer in both crystals, corresponding to a Matthews coefficient (V_M) of 2.37 Å^3 Da^{-1} and a solvent content of 48.0%.

1. Introduction

Succinic semialdehyde dehydrogenase (SSADH) plays an essential role in mammalian neurobiology and is involved in the turnover of γ-aminobutyric acid (GABA), which is the last step of the GABA shunt. GABA is directly synthesized from glutamate and is a major inhibitory neurotransmitter in the central nervous system (de Carvalho *et al.*, 2011). GABA-transaminase catalyzes the breakdown of GABA in the presence of α-ketoglutarate to produce succinic semialdehyde (SSA). SSA is then converted to succinic acid (SA) by SSADH (Jakoby & Scott, 1959). Hence, GABA is channelled into the tricarboxylic acid cycle in the form of SA for further metabolism. However, the roles of the GABA shunt and SSADH in bacteria have been less studied than in mammals. In bacteria, GABA has been associated with glutamate metabolism, anaplerosis and/or antioxidant defence (de Carvalho *et al.*, 2011).

Aldehyde dehydrogenases (ALDHs) are a group of enzymes that catalyze the conversion of aldehydes to their corresponding acids by means of a virtually irreversible NAD(P)$^+$-dependent reaction. The most widely studied ALDHs are known to exist in dimeric or tetrameric states (Yoshida *et al.*, 1998). Many such enzymes are involved in cellular detoxification and cellular differentiation (Cobessi *et al.*, 1999). SSADH belongs to the ALDH superfamily (Chambliss *et al.*, 1995) and has been identified and purified from mammals (Blaner & Churchich, 1980; Chambliss & Gibson, 1992; Lee *et al.*, 1995; Ryzlak & Pietruszko, 1988) and from microorganisms (Donnelly & Cooper, 1981; Koh *et al.*, 1994; Sanchez *et al.*, 1989). Bacterial SSADHs vary in their cofactor preference and two distinct SSADHs were first described in *Pseudomonas fluorescens* (Jakoby & Scott, 1959). In *Escherichia coli*, two SSADH genes, the *gabD* and *sad* genes, have been identified (Skinner & Cooper, 1982). The *gabD* gene encodes an NADP$^+$-dependent SSADH (EC 1.2.1.24) and is located in the *gab* operon. The *sad* gene encodes an NAD$^+$/NADP$^+$-dependent SSADH (EC 1.2.1.16) that shares 32% identity with *gabD* and is an orphan gene (Fuhrer *et al.*, 2007).

The Gram-positive bacterium *Streptococcus pyogenes* (group A streptococcus) is the most common pathogen causing upper respiratory tract and skin infections. It is also responsible for post-

streptococcal diseases such as rheumatic fever and glomerulonephritis, in addition to increasing the incidence of invasive infections such as streptococcal toxic shock syndrome (Cunningham, 2000). One serious problem that has recently been observed in *S. pyogenes* therapy is the attenuation of the effects of antibiotics, especially penicillin treatment failure and macrolide resistance (Minami *et al.*, 2011). Thus, the development of novel antibacterial drugs is now being sought.

Although several crystal structures of SSADH have been reported, the structures of SSADHs remain poorly studied in comparison to other dehydrogenases and with regard to the correlation between their cofactor preference and their distinct dimeric or tetrameric forms. SSADH from *S. pyogenes* shows approximately 32% sequence identity to human (PDB entry 2w8n; Kim *et al.*, 2009) and *E. coli* (PDB entry 3jz4; Langendorf *et al.*, 2010) SSADHs. Therefore, more detailed investigations are required in order to compare the existing structures of SSADHs and to improve the understanding of their metabolic function. As the first step towards the elucidation of its structure, we report the crystallization and preliminary X-ray crystallographic analysis of SSADH from *S. pyogenes* in native and complexed forms.

2. Materials and methods

2.1. Cloning and protein expression

The gene encoding SSADH was amplified by polymerase chain reaction (PCR) from *S. pyogenes* genomic DNA using the forward primer 5′-GCG CCG **CAT ATG** GCT TAT CAA ACT ATT TAC-3′ and the reverse primer 5′-GGG CCG **CTC GAG** TCA AAC TTT AGT ATT GCC-3′ (*Nde*I and *Xho*I recognition sites are shown in bold). The PCR-amplified DNA fragment was then digested with *Nde*I and *Xho*I and inserted into the bacterial expression vector pET-28a (Novagen, USA) to generate the plasmid pSpSSADH consisting of *S. pyogenes* SSADH (SpSSADH) with six consecutive histidines at the N-terminus. *E. coli* BL21 (DE3) cells (Novagen, USA) harbouring pSpSSADH were grown in Luria–Bertani medium with 50 µg ml^{-1} kanamycin at 310 K to an optical density at 600 nm of 0.6. Protein expression was induced by addition of 0.5 m*M* isopropyl β-D-1-thiogalactopyranoside and incubation at 310 K for a further 4 h. The cells were harvested by centrifugation at 5000*g* for 30 min at 277 K.

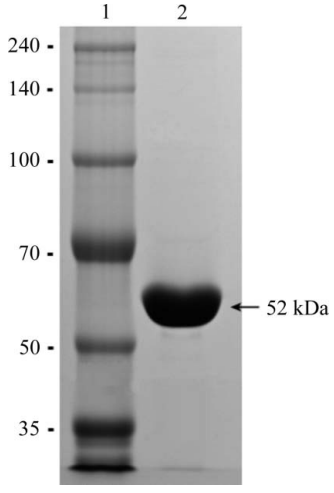

Figure 1
SDS–PAGE of SpSSADH. Lane 1, molecular-weight markers (labelled in kDa); lane 2, purified SpSSADH protein.

2.2. Protein purification

The harvested cell pellets were suspended in buffer *A* (20 m*M* Tris–HCl pH 7.9, 500 m*M* NaCl, 5 m*M* imidazole) and disrupted by sonication at 277 K. The crude lysate was centrifuged at 25 000*g* for 30 min at 277 K. The supernatant was loaded onto an Ni^{2+}-chelated HiTrap chelating HP column (GE Healthcare, USA) equilibrated in buffer *A*. The bound protein was eluted with a linear gradient of buffer *B* (20 m*M* Tris–HCl pH 7.9, 500 m*M* NaCl, 1 *M* imidazole). Fractions containing SpSSADH were identified by SDS–PAGE and subsequently purified by gel-filtration chromatography on a HiLoad 16/60 Superdex 200 column (GE Healthcare, USA) which had been equilibrated with gel buffer (30 m*M* Tris–HCl pH 7.5, 100 m*M* NaCl, 10 m*M* β-mercaptoethanol, 5% glycerol). The soluble fractions containing protein were pooled together and concentrated to 26 mg ml^{-1} using an Amicon Ultra-15 centrifugal filter device (Millipore, USA). This procedure yielded approximately 85 mg SpSSADH protein from a 1 l culture. The protein concentration was estimated using the Bradford assay and the purity was confirmed by 15% SDS–PAGE to be >95% (Fig. 1).

2.3. Crystallization and preliminary X-ray analysis

Preliminary crystallization screening for the SpSSADH enzyme was performed *via* the sitting-drop vapour-diffusion method (0.5 µl protein solution and 0.5 µl reservoir solution equilibrated against 50 µl reservoir solution) using various commercial screening kits (Crystal Screen, Crystal Screen 2, PEGRx 1 and 2, SaltRx 1 and 2 from Hampton Research, USA and Morpheus from Molecular Dimensions, UK) in 96-well Intelli-Plates (Art Robbins Instruments, USA) at 295 K. Initial crystals were obtained using the following condition: 0.1 *M* MES monohydrate pH 6.0, 14%(*w*/*v*) polyethylene glycol 4000 (from PEGRx 1; Hampton Research, USA). Crystal growth was optimized using the hanging-drop vapour-diffusion

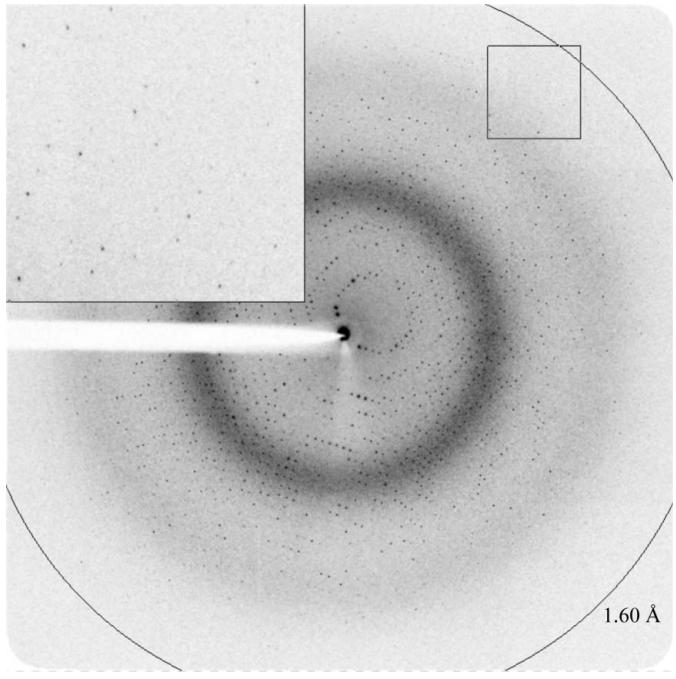

Figure 2
X-ray diffraction pattern of a native SpSSADH crystal obtained using a Rigaku/MSC Jupiter210 CCD detector. The box shows an enlargement of an area containing high-resolution spots.

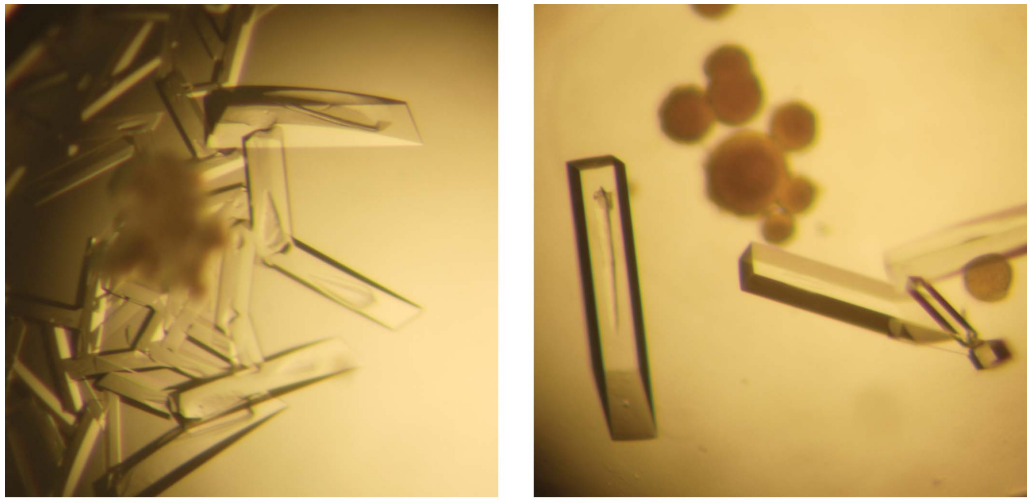

(*a*) (*b*)

Figure 3
Crystals of the SSADH protein from *S. pyogenes*. (*a*) Native SpSSADH crystals; (*b*) SpSSADH–NAD$^+$ complex crystals. The crystal dimensions are approximately 0.8 × 0.3 × 0.1 mm for the native crystals and 1.0 × 0.2 × 0.2 mm for the SpSSADH–NAD$^+$ complex crystals.

Table 1
Data-collection statistics.

Values in parentheses are for the highest resolution shell.

	Native	NAD$^+$ complex
Space group	$P2_12_12_1$	$P2_12_12_1$
Unit-cell parameters (Å, °)	a = 93.3, b = 100.3, c = 105.1	a = 93.3, b = 100.3, c = 105.0
Resolution range (Å)	50–1.6 (1.63–1.60)	50–1.7 (1.73–1.70)
Total/unique reflections	1262499/128443	934181/108229
Mosaicity (°)	0.37	0.47
Multiplicity	9.8 (4.8)	8.6 (4.2)
Completeness (%)	98.5 (88.4)	99.5 (97.1)
$R_{\rm merge}$† (%)	7.1 (30.6)	9.6 (41.0)
$\langle I/\sigma(I)\rangle$	26.3 (2.5)	16.8 (1.7)

† $R_{\rm merge} = \sum_{hkl}\sum_i |I_i(hkl) - \langle I(hkl)\rangle| / \sum_{hkl}\sum_i I_i(hkl)$, where $I_i(hkl)$ represents the ith observed intensity of reflection hkl and $\langle I(hkl)\rangle$ represents the average intensity of reflection hkl.

method in 24-well XRL plates (Molecular Dimensions, UK); each drop was made up of 1 µl protein solution and 1 µl reservoir solution [0.1 *M* MES monohydrate pH 5.8–6.1 and 18–23%(*w*/*v*) polyethylene glycol 4000] and was equilibrated over 500 µl reservoir solution. For cocrystallization, the protein solution was mixed with NAD$^+$ in a 1:10 molar ratio. The NAD$^+$-complex crystals were obtained using the same conditions as were used for the native crystal. The crystals were transferred into a cryoprotection solution consisting of 25% ethylene glycol in reservoir solution. The cryoprotected crystals were then directly flash-cooled at 100 K in a stream of nitrogen gas. Data sets were collected from the native SSADH and the SSADH–NAD$^+$ complex crystals on beamline BL26B1 at SPring-8 (Hyogo, Japan) using a Rigaku/MSC Jupiter210 CCD detector. A total range of 360° was covered using 1.0° oscillations and 1 s exposure per frame for the native crystal and 2 s exposure per frame for the SSADH–NAD$^+$ complex crystal. The wavelength of the synchrotron X-ray beam was 1.0000 Å. The crystal-to-detector distance was set to 150 mm. The X-ray diffraction data showed that the native crystal diffracted to 1.6 Å resolution and the SpSSADH–NAD$^+$ complex crystal diffracted to 1.7 Å resolution (Fig. 2). All data sets were indexed, integrated and scaled using the *HKL*-2000 software package (Otwinowski & Minor, 1997).

3. Results and discussion

The gene encoding the SSADH protein from *S. pyogenes* was successfully cloned, expressed in *E. coli* BL21 (DE3) and purified with an N-terminal His_6 tag by two steps of column chromatography: Ni^{2+}-affinity and gel-filtration chromatography. The molecular weight of SpSSADH was predicted to be 52 kDa from the sequence and this was confirmed by SDS–PAGE. Crystals suitable for X-ray diffraction were obtained using an optimized reservoir solution consisting of 0.1 *M* MES monohydrate pH 6.0 and 21%(*w*/*v*) polyethylene glycol 4000 for both the native and NAD$^+$-complex crystals. Suitable-sized crystals were obtained within 7 d and were used for X-ray diffraction. The crystal dimensions of native and NAD$^+$-complexed crystals were approximately 0.8 × 0.3 × 0.1 and 1.0 × 0.2 × 0.2 mm, respectively (Fig. 3).

The native crystal of SpSSADH diffracted to a resolution of 1.6 Å and belonged to the orthorhombic space group $P2_12_12_1$, with unit-cell parameters a = 93.3, b = 100.3, c = 105.1 Å. The crystal of the SpSSADH–NAD$^+$ complex diffracted to a resolution of 1.7 Å and also belonged to space group $P2_12_12_1$, with unit-cell parameters a = 93.3, b = 100.3, c = 105.0 Å. In both crystals the asymmetric unit contained one dimer, corresponding to a $V_{\rm M}$ value of 2.37 Å^3 Da^{-1}, with an estimated solvent content of 48.0% (Matthews, 1968). Data-collection statistics are summarized in Table 1. Structure determination of SpSSADH was performed by the molecular-replacement method using the *CNS* program (Brünger *et al.*, 1998; Brunger, 2007) with *E. coli* SSADH (PDB entry 3jz4; Langendorf *et al.*, 2010) as the search model. The results of molecular replacement clearly confirmed that the preliminary solution of the model structure contains one dimer in the asymmetric unit. Further refinement of the model structures is currently in progress and the structural details will be reported separately.

We thank the staff of the BL26B1 beamline at Spring-8, Japan for assistance during X-ray data collection.

References

Blaner, W. S. & Churchich, J. E. (1980). *Eur. J. Biochem.* **109**, 431–437.
Brunger, A. T. (2007). *Nature Protoc.* **2**, 2728–2733.

Brünger, A. T., Adams, P. D., Clore, G. M., DeLano, W. L., Gros, P., Grosse-Kunstleve, R. W., Jiang, J.-S., Kuszewski, J., Nilges, M., Pannu, N. S., Read, R. J., Rice, L. M., Simonson, T. & Warren, G. L. (1998). *Acta Cryst.* D**54**, 905–921.
Carvalho, L. P. de, Ling, Y., Shen, C., Warren, J. D. & Rhee, K. Y. (2011). *Arch. Biochem. Biophys.* **509**, 90–99.
Chambliss, K. L., Caudle, D. L., Hinson, D. D., Moomaw, C. R., Slaughter, C. A., Jakobs, C. & Gibson, K. M. (1995). *J. Biol. Chem.* **270**, 461–467.
Chambliss, K. L. & Gibson, K. M. (1992). *Int. J. Biochem.* **24**, 1493–1499.
Cobessi, D., Tête-Favier, F., Marchal, S., Azza, S., Branlant, G. & Aubry, A. (1999). *J. Mol. Biol.* **290**, 161–173.
Cunningham, M. W. (2000). *Clin. Microbiol. Rev.* **13**, 470–511.
Donnelly, M. I. & Cooper, R. A. (1981). *J. Bacteriol.* **145**, 1425–1427.
Fuhrer, T., Chen, L., Sauer, U. & Vitkup, D. (2007). *J. Bacteriol.* **189**, 8073–8078.
Jakoby, W. B. & Scott, E. M. (1959). *J. Biol. Chem.* **234**, 937–940.
Kim, Y.-G., Lee, S., Kwon, O.-S., Park, S.-Y., Lee, S.-J., Park, B.-J. & Kim, K.-J. (2009). *EMBO J.* **28**, 959–968.
Koh, Y. S., Joo, C. N., Choi, S. Y. & Kim, D. S. (1994). *Korean Biochem. J.* **27**, 75–79.
Langendorf, C. G., Key, T. L., Fenalti, G., Kan, W. T., Buckle, A. M., Caradoc-Davies, T., Tuck, K. L., Law, R. H. & Whisstock, J. C. (2010). *PLoS One*, **5**, e9280.
Lee, B. R., Hong, J. W., Yoo, B. K., Lee, S. J., Cho, S. W. & Choi, S. Y. (1995). *Mol. Cells*, **5**, 611–617.
Matthews, B. W. (1968). *J. Mol. Biol.* **33**, 491–497.
Minami, M., Ichikawa, M., Hata, N. & Hasegawa, T. (2011). *PLoS One*, **6**, e22188.
Otwinowski, Z. & Minor, W. (1997). *Methods Enzymol.* **276**, 307–326.
Ryzlak, M. T. & Pietruszko, R. (1988). *Arch. Biochem. Biophys.* **266**, 386–396.
Sanchez, M., Fernández, J., Martin, M., Gibello, A. & Garrido-Pertierra, A. (1989). *Biochim. Biophys. Acta*, **990**, 225–231.
Skinner, M. A. & Cooper, R. A. (1982). *Arch. Microbiol.* **132**, 270–275.
Yoshida, A., Rzhetsky, A., Hsu, L. C. & Chang, C. (1998). *Eur. J. Biochem.* **251**, 549–557.